J. Am. Soc. Mass Spectrom. (2013) 24:1988–1996
DOI: 10.1007/s13361-013-0732-8

RESEARCH ARTICLE

Charge Enhancement of Single-Stranded DNA in Negative Electrospray Ionization Using the Supercharging Reagent Meta-nitrobenzyl Alcohol

Bessem Brahim, Sandra Alves, Richard B. Cole, Jean-Claude Tabet

Institut Parisien de Chimie Moléculaire, Equipe de Chimie Structurale Organique et Biologique, Université Pierre et Marie Curie, CNRS UMR 7201, 75252 Paris cedex 05, France

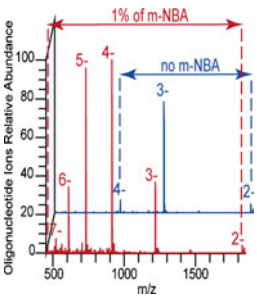

Abstract. Charge enhancement of single-stranded oligonucleotide ions in negative ESI mode is investigated. The employed reagent, meta-nitrobenzyl alcohol (m-NBA), was found to improve total signal intensity (I_{tot}), increase the highest observed charge states (z_{high}), and raise the average charge states (z_{avg}) of all tested oligonucleotides analyzed in negative ESI. To quantify these increases, signal enhancement ratios ($SER_{1\%}$) and charge enhancement coefficients ($CEC_{1\%}$) were introduced. The $SER_{1\%}$, (defined as the quotient of total oligonucleotide ion abundances with 1 % m-NBA divided by total oligonucleotide abundance without m-NBA) was found to be greater than unity for every oligonucleotide tested. The $CEC_{1\%}$ values (defined as the average charge state in the presence of 1 % m-NBA minus the average charge state in the absence of m-NBA) were found to be uniformly positive. Upon close inspection, the degree of charge enhancement for longer oligonucleotides was found to be dependent upon thymine density (i.e., the number and the location of phospho-thymidine units). A correlation between the charge enhancement induced by the presence of m-NBA and the apparent gas-phase acidity (largely determined by the sequence of thymine units but also by the presence of protons on other nucleobases) of multiply deprotonated oligonucleotide species, was thus established. Ammonium cations appeared to be directly involved in the m-NBA supercharging mechanism, and their role seems to be consistent with previously postulated ESI mechanisms describing desorption/ionization of single-stranded DNA into the gas phase.

Key words: Supercharging, Single-stranded DNA, Meta-nitrobenzyl alcohol, Electrospray, Gas-phase acidity, Apparent gas-phase acidity, Ammonium counter-ion, Desolvation

Received: 10 July 2012/Revised: 26 July 2013/Accepted: 7 August 2013/Published online: 13 September 2013

Introduction

Almost since the discovery of multiple charging of protein molecules by electrospray ionization [1], mass spectrometrists have been trying to understand and manipulate the charge state distributions that one may obtain [2]. The shift in charge state distributions was shown to be dramatic when proteins passed from their native folded states to denatured extended conformations as solution pH was lowered [3]. However, the effect of pH on charge state distributions was much more subtle when small peptides that were not susceptible to "unfolding" were subjected to extreme pH variations [4]. Other solution additives such as nitrogen bases were shown to influence charge state distributions by creating a competition between basic sites bearing excess protons on an analyte protein and the small nitrogen base adducted to this charged site [5, 6]. For example, when introduced as a formate or acetate salt, the ammonium cation (NH_4^+) will act largely as a protonating agent in the presence of highly basic amino acids. In addition to the above solution-phase considerations, in the early 1990s, gas-phase charge manipulation was achieved by reacting dimethylamine with multiply protonated cytochrome *c* [7], or 1,6-diaminohexane with multiply protonated myoglobin in an ion trap mass spectrometer [8]. These gas-phase studies resulted in a reduction in the overall

Correspondence to: Jean-Claude Tabet ; *e-mail:* jean-claude.tabet@ipcm.upmc.fr

charge of protein species as protons were transferred to the introduced bases.

In the beginning of the 21st century, meta-nitrobenzyl alcohol (m-NBA), previously used as a matrix to improve desorption/ionization processes in fast atom bombardment mass spectrometry [9–12], was proposed as a supercharging reagent in positive ion electrospray mass spectrometry (ESI-MS) by Williams and co-workers [13–16]. Through these studies, they showed not only the ability of m-NBA to enhance both the highest observed (z_{high}) and average (z_{avg}) charge states of multiply protonated proteins [13–16] and peptides [13], but also its ability to favor higher charge states of cationized synthetic organic polymers (e.g., PEG 1500, [14, 15] in ESI positive ion mode). They reported a limited influence of m-NBA on oxidized insulin chain A under negative ESI conditions [14]. Access to higher charge states allows analysis of larger biological systems when the *m/z* range of the mass spectrometer is limited; the achievable mass resolution may also increase for mass analyzers that exhibit decreasing resolving power at higher *m/z* values (e.g., Fourier transform ion cyclotron resonance. Electron capture efficiency may also be augmented at higher charge states [17–19].

From its introduction, many attempts have been made to better understand how the chemical characteristics of m-NBA lead to supercharging. Among the properties considered are surface tension [13–16, 20–22], vapor pressure (or boiling point) [14–16, 20–26], gas-phase basicity [14, 16, 20–25, 27–29], etc. According to the work of Kebarle et al. [6, 30, 31], these properties can be divided into two groups corresponding to the progressive steps of evaporation/desolvation in ESI. Vapor pressure and surface tension are important physico-chemical properties starting from the macroscopic early phases of the charged droplet's lifetime. On the other hand, solvent-free (or sparsely solvated) charged molecular species appear only at the very end of the charged droplet's lifetime, so Gibbs free energy change of protonation/deprotonation reactions [i.e., GB for positive ion production and ΔG°(acid) for negative ion production] intervene directly only at this stage of desolvation in the ESI process. Because the vapor pressure of m-NBA (b_p = 177 °C at 3 Torr [32]) is lower than that of water (b_p = 100 °C at 766 Torr [32]), a noticeable influence of m-NBA on ESI charge states is observed in aqueous solutions even at very low reagent concentrations [14–16, 20–28, 33]. This is because during the course of water molecule evaporation, the concentration of supercharging reagent increases until it becomes the most abundant solvent species present into the final droplets [14]. The high concentration of reactive aromatic molecules remaining after water evaporation could induce conformational changes of studied macromolecules, *e.g.* proteins [13–16, 20, 25] and protein noncovalent complexes [21–24, 26–28, 33]. Lower vapor pressure also implies a slower droplet cool down that could favor conformational changes of biomolecules due to their higher internal energy [22, 24].

During the last few years, protein possible conformational changes have been studied using denaturation conditions induced by solvent [29, 34, 35] or temperature variations [22, 24], but also by employing a reversed strategy (i.e., by chemically "locking" the protein tertiary structure with introduced covalent linkages [28]. As expected, the presence of m-NBA did not modify the existing correlation trend for biomolecular species (i.e., the more unfolded the protein is, the more charges it can carry [24, 27–29]. But it has not yet been clarified whether (1) the presence of additional charged sites causes increased Coulombic repulsion leading to protein unfolding or (2) protein unfolding induced by the presence of m-NBA reveals new accessible protonable sites, which lead to the observed charge state enhancement. Even if the GB value of m-NBA in positive ion mode has been implicated as a major thermochemical property responsible for these trends [23, 29, 33], conformational changes of the analyte (that may or may not occur in response to the presence of m-NBA) hinder the ability to unambiguously assign the underlying reasons for the success of m-NBA as a supercharging reagent.

In the current study, we examine the influence of m-NBA reagent in negative ESI ion mode on oligonucleotide charge state distributions [36]. The several phosphate groups present on the oligonucleotide backbone and, thus, the acidic character of single-stranded DNA (ssDNA) explains why these compounds have mostly been studied in the negative ion mode [37–43]. Positive ion studies of DNA are also possible [43–49] owing to the substantial GB values of nucleobases that are readily protonated in solution with counter-ions (e.g., deprotonated solvent molecules, nearby. Ammonium acetate, commonly used as buffer for ssDNA samples, does not only control the pH of the solution (e.g., preventing further duplex production), it also interacts with phosphate groups that are fully deprotonated in solution (pKa < 1) and, thus, induces a competition between NH_4^+ and alkali metals for the role of counter-ion. After complete evaporation of the solvent, and during the desolvation step in the microscopic state, intermolecular proton transfer(s) could occur between oligonucleotide anions and NH_4^+ cations leading to fewer deprotonated sites on the oligonucleotides [43]. Since ammonia (NH_3) is not basic enough to form stable salt bridges with phosphate groups [50], such proton transfers are most likely to occur during the last stages of ESI desolvation and are guided by the respective GB of NH_3 (819 $kJ.mol^{-1}$, [51]) and the apparent Gibbs free energy change ($\Delta G°_{app}$[acid]) of the deprotonation reaction of multiply deprotonated oligonucleotide species ($[DNA-nH]^{n-}$). An excess of ammonium acetate can shift the charge state distribution of $[DNA-nH]^{n-}$ toward lower n values by favoring departures of NH_3 molecules (leaving behind the proton) and resulting in a decrease in the number of negative charges located on the ssDNA backbone [52]; z_{avg} of oligonucleotide anions are strongly dependent upon the $\Delta G°_{app}$(acid) of $[DNA-nH]^{n-}$ and, thus, upon oligonucleotide sequence, especially the density (i.e., number and consecutivity) of phosphor-thymidine units [53]

(the most acidic nucleotide [50, 54–56]). Madsen and Brodbelt [57] have observed the charge enhancement of duplexes in negative ESI-MS induced by the presence of m-NBA, but the enhancement was accompanied by in-source dissociations into the corresponding ssDNA. Since no predefined conformations of single-stranded oligonucleotides have been established as being predominant for short sequences [58–60], the presence of m-NBA would not be expected to induce conformational changes that could potentially alter the number of apparent deprotonable sites of ssDNA. Because of the elimination of this conformational factor from the mechanistic interpretation of the influence of m-NBA, the use of oligonucleotides can perhaps give more precise information than proteins on m-NBA's specific role in charging during ESI.

Experimental

Sample Preparation

ssDNA (12-mer: 5′-AAAAACCAAAAA-3′, 5′-TTGGTTAATTCC-3′, 5′-GGAATTAACCAA-3′, 5′-GGTTAATTCCTT-3′, 5′-CCAATTAAGGAA-3′, 5′-GGCCACAATTT-3′, 5′-AAATTGTGGCCC-3′, 5′-CCCTTGTGGAAA-3′, 5′-TTTCCACAAGGG-3′, 5′-TTTTTGGTTTGG-3′, and 6-mer: 5′-TTTTTT-3′, 5′-TTATTT-3′, 5′-TTCTTT-3′, 5′-GTTTTT-3′, 5′-GGGTTT-3′) with 5′ and 3′ hydroxyl terminal groups were obtained from EUROFINS MWG Biotech (Ebersberg, Germany) and were used without further purification. All other chemicals were purchased from Sigma-Aldrich Chemicals (St. Quentin Fallavier, France). All solutions were prepared using deionized water (10 MΩ) with 20 mM ammonium acetate, HPLC grade methanol (50:50, vol/vol) and with or without addition of 1 % volume of m-NBA. Oligonucleotide solutions at 20 µM were injected into the instrument at a flow rate of 5 $\mu L.min^{-1}$.

Mass Spectrometry

Experiments were performed using an electrospray ionization source in negative ion mode combined with an LTQ-Orbitrap hybrid instrument (Thermo Scientific, San Jose, CA, USA) [61–63]. ESI conditions were as follows: accelerating voltage 3.5 kV; ion transfer tube temperature 280 °C; capillary voltage –50 V; and tube lens voltage –110 V. Nitrogen was used as sheath gas and auxiliary gas. High resolution mass spectra (*m/z* 200–2000) were acquired in the Orbitrap cell (theoretical mass resolving power of 60 000 at *m/z* 400), after external ion accumulation. The resolution power and mass accuracy allow the observation of the isotopic profile and facilitate the identification of molecular species and their resulting charge states. All data were acquired using external calibration. Relative standard deviations (RSD) were calculated from 10 repeated measurements and are presented in the respective tables.

Results

To gain insight into the influence of $\Delta G°_{app}$(acid) of $[DNA - nH]^{n-}$ on m-NBA's action towards oligonucleotide charging processes, various DNA sequences and sizes (from 6- to 12-mer) were examined.

Figures 1 and 2 present negative mode ESI mass spectra of 5′-GTTTTT-3′ and 5′-GGAATTAACCAA-3′ solutions, respectively. Comparison of mass spectra obtained without (Figures 1a and 2a) or with (Figures 1b and 2b) addition of m-NBA, clearly shows the effect of m-NBA on the charge state distribution of oligonucleotide ions. The presence of m-NBA has broadened the charge state distribution of oligonucleotide ions, from 1 to 4 charge states for the 6-mer (Figure 1), and from 3 to 7 charge states for the 12-mer (Figure 2). In addition to this widening of the charge state distributions, the presence of m-NBA has dramatically increased the z_{high} of smaller oligonucleotide ions from –2 to –5; the –5 charge state obtained with m-NBA corresponds to the deprotonation of all phosphate groups constituting the 6-mer ssDNA and, therefore, to the maximum potential charge state (z_{max}) (Figure 1). The same trend has been observed for longer oligonucleotides, shifting the z_{high} from –4 to –8 corresponding to the deprotonation of 8 out of the 11 phosphate groups constituting the 12-mer ssDNA (Figure 2). For all tested oligonucleotides, the lowest observed charge state (z_{low}) stayed the same despite the presence of m-NBA. Note that "satellite" peaks present in Figure 1b correspond to alkali metal adducts, whereas no m-NBA adducts of oligonucleotides were observed.

Figure 3 presents positive ion mass spectra of 5′-TTTTTGGTTTGG-3′ solutions. Comparison of mass spectra obtained without (Figure 3a) or with (Figure 3b) addition of m-NBA shows a relatively minor effect on the charge state distribution of oligonucleotide ions observed in positive ESI mode.

Both z_{high} and z_{low} stayed the same while the ion abundance ratio z_{high}/z_{low} has slightly decreased in the presence of m-NBA.

Tables 1 and 2 present negative mode ESI results obtained for all tested oligonucleotide solutions in the absence and presence of 1 % m-NBA. Total oligonucleotide ion abundances (I_{tot}) have been calculated by summing the peak intensities of the entire natural isotopic cluster for each ion charge state. Two clear trends were deduced. First, a slight signal enhancement was observed for all tested oligonucleotides of any length or sequence. In order to quantify this signal enhancement that 1 % m-NBA induces on oligonucleotide ions, a "signal enhancement ratio" ($SER_{1\%}$) is defined as the quotient:

$$SER_{1\%} = \frac{I_{tot} in\ the\ presence\ of\ m{-}NBA}{I_{tot} in\ the\ absence\ of\ m{-}NBA} \quad (1)$$

Very importantly, in negative ESI mode, it was consistently found that all measured $SER_{1\%}$ quotients were higher

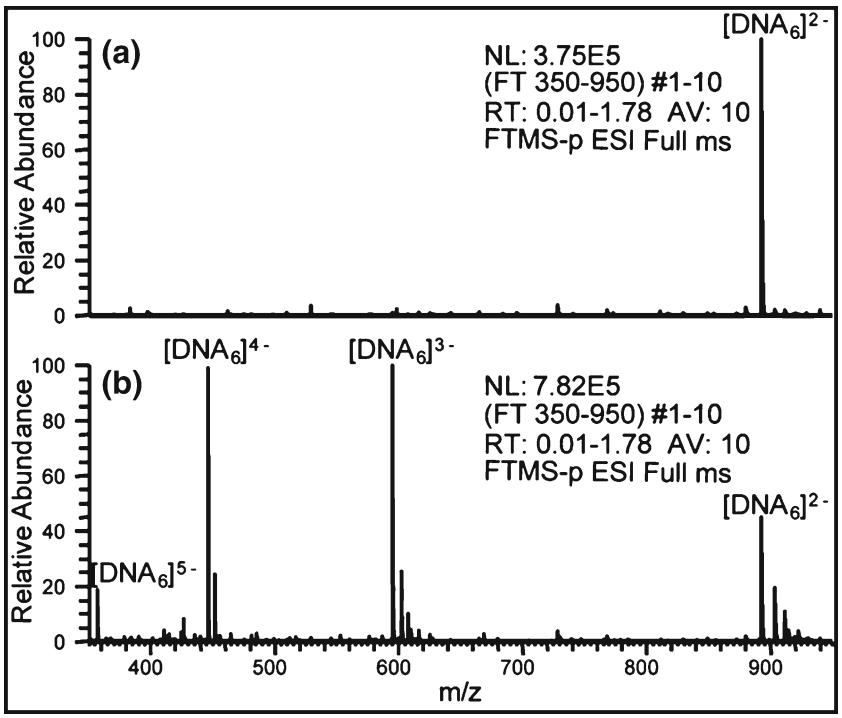

Figure 1. Mass spectra of 6-mer ssDNA ions (GTTTTT) in negative ESI mode, **(a)** without m-NBA and **(b)** with 1 % of m-NBA

than 1.0, indicating that the presence of 1 % m-NBA invariably resulted in signal enhancement (Table 1).

The second clear trend relates to shifts in the charge state distribution (Table 2). To evaluate the latter shift, average

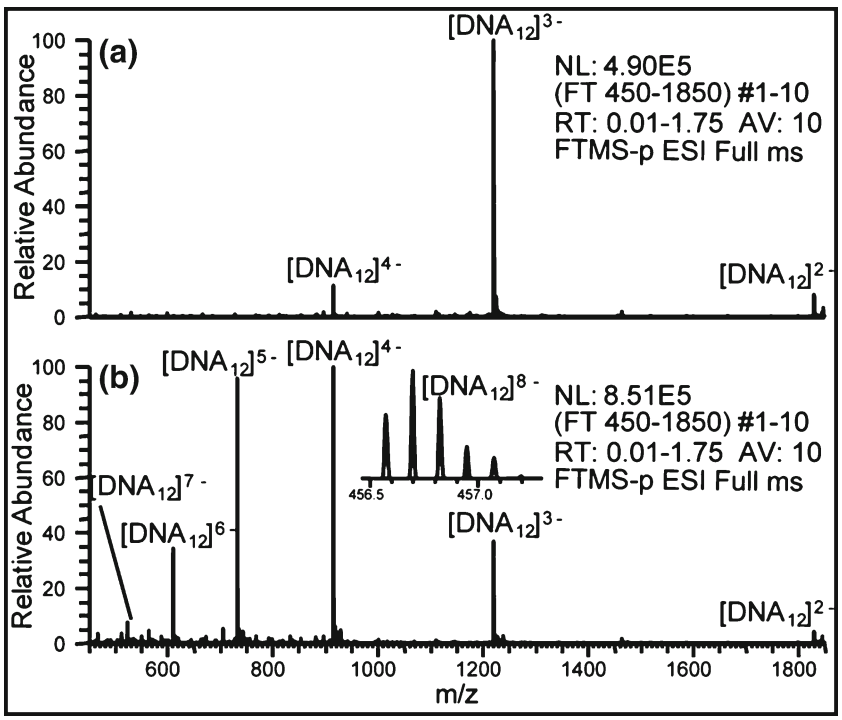

Figure 2. Mass spectra of 12-mer ssDNA ions (GGAATTAACCAA) in negative ESI mode, **(a)** without m-NBA and **(b)** with 1 % of m-NBA

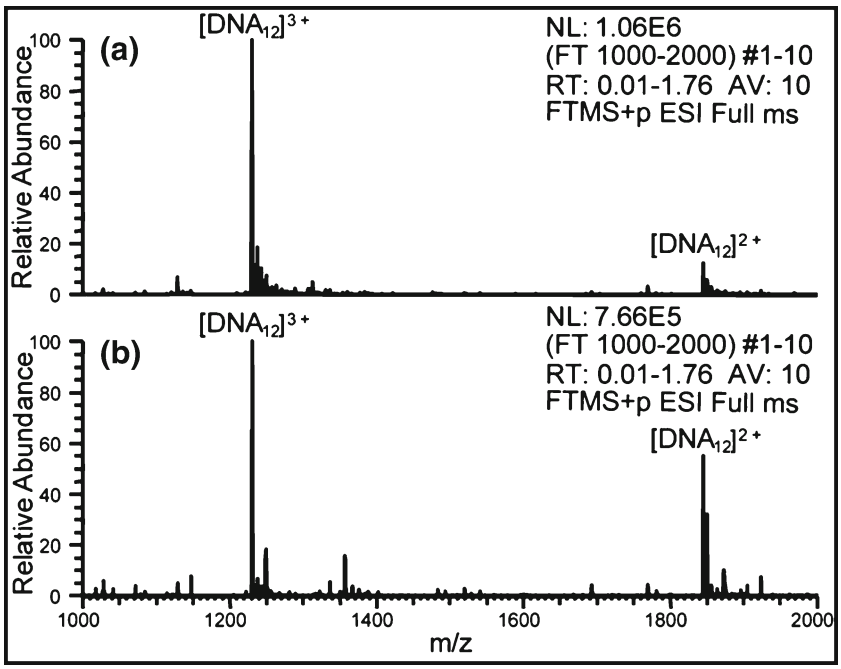

Figure 3. Mass spectra of 12-mer ssDNA ions (TTTTTGGTTTGG) in positive ESI mode, **(a)** without m-NBA and **(b)** with 1 % of m-NBA

charge states, z_{avg}, were calculated using the following formula [64]:

$$z_{avg} = \sum_{i}^{n} \frac{(i \; I^{i-})}{I_{tot}} \tag{2}$$

corresponding to the sum of each oligonucleotide ion abundance (I^{i-}) for a given charge state multiplied by its the charge state value (i), divided by the sum of all oligonucleotide ion abundances (I_{tot}). A clear increase of z_{avg} values was observed for all tested ssDNA after m-NBA addition, independently of the oligonucleotide length or sequence.

To better quantify the shift in charge states induced by 1 % m-NBA addition, a charge enhancement coefficient ($CEC_{1\%}$) is defined as:

$$CEC_{1\%} = \left(z_{avg} in \; presence \; of \; m\text{–}NBA\right) - \left(z_{avg} in \; absence \; of \; m\text{–}NBA\right) \tag{3}$$

The utility of this charge enhancement coefficient is that it allows a direct assessment of the influence of m-NBA addition (i.e., initial variability in charge state distributions is subtracted out. Very importantly, all calculated $CEC_{1\%}$ values were found to be strictly positive, showing the ability of m-NBA to enhance z_{avg} of $[DNA - nH]^{n-}$ ions. Additionally, $CEC_{1\%}$ values obtained for larger oligonucleotides are shown to increase with the number of thymine units; moreover, small shifts are observed depending upon the thymine location.

Discussion

Through the last decade, m-NBA was extensively described in the literature for its ability to enhance, in positive ESI ion mode, the signal intensity [14], z_{high} and z_{avg} [13–16, 20–29, 33, 34] of peptides [13, 20, 25], proteins [13–16, 23, 25–29, 34], and noncovalent protein complexes [21, 22, 24, 33]. Early on, Williams and co-workers [15] proposed that the solvent surface tension is an important macroscopic factor involved in the supercharging mechanism. Indeed, the Rayleigh limit for a spherical droplet is classically given by:

$$z_r e = 8\pi\left(\varepsilon_0 \; \gamma \; R^3\right)^{1/2} \tag{4}$$

where, z_r is the unit charge limit, e is the elementary charge, ε_0 is the permittivity of the surrounding medium, γ is the surface tension, and R is the droplet radius. The overall surface tension modification induced by addition of m-NBA and the resulting Rayleigh charge limit are presumably independent of the studied polarity. Therefore, the enhancements should be observed regardless of the ion polarity when the same sample preparation and experimental conditions are employed within the limits of the analyte's ability to undergo proton exchange processes. Attempts performed in negative ion ESI on amphoteric proteic ions, such as the oxidized A chain of insulin [14] or myoglobin noncovalent complexes [24], have only yielded slight increases in z_{avg}.

However, for all tested oligonucleotides in positive ESI mode, $SER_{1\%}$ values were measured to be less than 1.0, thereby revealing a decrease of $[DNA + H]^{n+}$ ion abundance

in the presence of m-NBA (Figure 3). Accordingly, $CEC_{1\%}$ values were found to be strictly negative under these conditions, showing a decrease of z_{avg} values in the presence of m-NBA (Figure 3). This contrast in results obtained for the two ion polarities shows that solvent surface tension is likely to not be the only factor involved in the supercharging mechanism of oligonucleotides. It is our view that the contradicting experimental results obtained in each polarity are likely indicative of the charging mechanism of DNA. No matter which ion polarity is used, the outcome of m-NBA addition on the oligonucleotide ionization resulted in a consistent decrease in the number of net positive charges (positive ion mode) or, similarly, an increased number of net negative charges (negative ion mode). This evidence supports the notion that m-NBA promotes a unidirectional intermolecular proton transfer ending in a higher number of deprotonated phosphate groups regardless of ion polarity.

For proteins, Loo and co-workers have shown that since (1) no protonated m-NBA reagent is observed in the low *m/z* region, and (2) m-NBA clustering onto proteins are lost as neutral m-NBA species (at higher transfer energies) while supercharging myoglobin ions in positive ESI mode, m-NBA has a lower GB than GB_{app} of $[Myo + nH]^{n+}$ [21, 23]. From the analogous observations in negative ESI mode (no $[m\text{-}NBA - H]^-$ or negatively charged oligonucleotide adducts with m-NBA observed because of the harsh ESI conditions used), it could be concluded either that m-NBA appears to have a higher $\Delta G°(acid)$ value than $\Delta G°_{app}(acid)$ of all observed $[DNA - nH]^{n-}$ species, or that m-NBA molecules do not interact directly with phosphate groups and need assistance to deprotonate ssDNA. Indeed, a signal loss has been observed when ammonium acetate buffer was not introduced during sample preparation. If a direct intermolecular proton exchange occurs between m-NBA and oligonucleotide ions during the last desolvation steps, the obtained charge enhancement should be observed even in the absence of NH_4^+ counter-ions. Effects induced by the presence of m-NBA could, therefore, be explained by the previously established conventional desolvation model for transfer of oligonucleotide ions from solution into the gas phase [43]. By definition, $\Delta G°(acid)$ values can be employed only when solvated ions (m-NBA/NH_4^+/ssDNA negatively charged aggregates) are released into the gas phase from micro-droplets (mostly composed of m-NBA because of its low vapor pressure compared with that of water). During the last desolvation steps, when NH_4^+ ions have the opportunity to leave a proton to a $[DNA - nH]^{n-}$ ion, the presence of m-NBA seems to facilitate the other competitive desolvation pathway involving the departure of an NH_4^+ cation rather than a neutral NH_3 molecule. This results in the creation of an additional negatively charged phosphate group on the oligonucleotide ion, and this process may occur more than once, until achieving a maximum level of deprotonation dictated by the $\Delta G°_{app}(acid)$ of $[DNA - nH]^{n-}$. When considering this type of consecutive deprotonation of an oligonucleotide, the $\Delta G°_{app}(acid)$ value of each successive multi-deprotonated anion increases progressively until the last thermochemically allowed intermolecular proton transfer, at which point the highest observable charge state (z_{high}) is reached. The width of the charge state distribution of oligonucleotides in the gas phase is thereby determined by the range of $\Delta G°_{app}(acid)$ values of $[DNA - nH]^{n-}$ between the first and the last intermolecular proton transfers. The propensity for such intermolecular proton transfers correlates with $\Delta G°_{app}(acid)$ values, which are dependent upon the specific DNA sequence and mostly upon the number of phospho-thymidine units (the most acidic nucleotide) present in the 12-mer ssDNA.

According to our model, the charge enhancement attributable to the presence of m-NBA occurs at the final stages of evaporation of the charged aggregated. The model can explain the difference in z_{avg} obtained in the presence or absence of m-NBA for oligonucleotide sequences of the same length (12-mers) containing different numbers of phospho-thymidine units (i.e., the most acidic nucleotide). With or without the presence of m-NBA, it was observed that z_{avg} values for oligonucleotide sequences containing three pairs of adjacent thymine units (i.e., three –TT- motifs) were higher than those obtained for sequences containing only one –TT- motif. For example, 5′-TTGGTTAATTCC-3′ and 5′-GGTTAATTCCTT-3′ oligonucleotide ions, respectively, exhibited z_{avg} values of (1) 3.119 and 3.133 without introduction of m-NBA, and (2) 4.71 and 4.73 with 1 % of m-NBA, whereas 5′-GGAATTAACCAA-3′ and 5′-CCAATTAAGGAA-3′ oligonucleotide ions have only yielded respectively z_{avg} values of: (1) 3.035 and 3.052 without m-NBA, and (2) 4.53 and 4.49 with 1 % of m-NBA. Additionally, $CEC_{1\%}$ values of $[DNA - nH]^{n-}$ followed the same trend (i.e., 1.59 and 1.60 for these same T-rich sequences compared with 1.49 and 1.43 for the sequences poorest in thymine units. Indeed, the presence of additional thymine nucleobases increases the number of preferentially deprotonable sites and, therefore, facilitates production of higher charge states of $[DNA - nH]^{n-}$. Thus, the first release of NH_4^+ occurs readily during desolvation (in preference to proton transfer to ssDNA), while further charging remains guided by the competition between NH_3/NH_4^+ releases from other nucleotide units (e.g., G, C, and A) i.e., by the $\Delta G°_{app}(acid)$ of $[DNA - nH]^{n-}$. For example, 5′-AAAAACCAAAAA-3′ oligonucleotide ion (containing no thymine) exhibited z_{avg} values of (1) 2.883 without introduction of m-NBA, and (2) 4.22 with 1 % of m-NBA; thus, a $CEC_{1\%}$ value of 1.34, which is the lowest value of the 12-mer set.

It is not only the number of thymine nucleobases that influence the charge enhancement induced by m-NBA, but also their locations in the DNA sequence play a role. Indeed, $CEC_{1\%}$ values obtained for 12-mer ssDNA sequences containing three consecutive thymine nucleobases (e.g., 1.38 and 1.41, respectively, for 5′-GGGCCACAATTT-3′ and 5′-TTTCCACAAGGG-3′ oligonucleotide ions) were found to be lower than those obtained for 12-mer ssDNA

Table 1. Total Ion Abundance (I_{tot}) Obtained Without or with Introduction of 1 % of m-NBA in Various ssDNA Solutions; Calculated Signal Enhancement Ratios ($SER_{1\%}$), Defined as the Quotient of I_{tot} with 1 % of m-NBA Divided by I_{tot} Without m-NBA. Relative Standard Deviations (RSD) were Calculated from 10 Different Measurements

	0 % m-NBA		1 % m-NBA		$SER_{1\%}$	RSD
	I_{tot}	RSD	I_{tot}	RSD		
6-mer						
5′-TTTTTT-3′	8.36×10^5	± 2 %	4.53×10^6	± 12 %	5.42	± 12 %
5′-TTATTT-3′	6.17×10^5	± 3 %	3.70×10^6	± 3 %	6.00	± 4 %
5′-TTCTTT-3′	6.55×10^5	± 2 %	4.41×10^6	± 3 %	6.74	± 3 %
5′-GTTTTT-3′	8.60×10^5	± 4 %	6.96×10^6	± 2 %	8.09	± 5 %
5′-GGGTTT-3′	5.61×10^5	± 1 %	6.25×10^6	± 2 %	11.15	± 2 %
12-mer						
5′-AAAAACCAAAAA-3′	2.47×10^6	± 5 %	8.30×10^6	± 1 %	3.34	± 5 %
5′-GGAA**TT**AACCAA-3′	1.94×10^6	± 2 %	7.67×10^6	± 1 %	3.94	± 3 %
5′-CCAA**TT**AAGGAA-3′	2.40×10^6	± 3 %	7.66×10^6	± 1 %	3.20	± 3 %
5′-GGGCCACAA**TTT**-3′	2.29×10^6	± 3 %	5.72×10^6	± 1 %	2.50	± 3 %
5′-**TTT**CCACAAGGG-3′	2.62×10^6	± 2 %	6.33×10^6	± 3 %	2.42	± 4 %
5′-AAA**TT**G**T**GGCCC-3′	2.13×10^6	± 4 %	6.37×10^6	± 3 %	2.98	± 5 %
5′-CCC**TT**G**T**GGAAA-3′	1.74×10^6	± 5 %	4.72×10^6	± 2 %	2.71	± 6 %
5′-**TT**GG**TT**AA**TT**CC-3′	1.61×10^6	± 8 %	9.30×10^6	± 2 %	5.76	± 8 %
5′-GG**TT**AA**TT**CC**TT**-3′	3.17×10^6	± 2 %	8.77×10^6	± 6 %	2.77	± 6 %

sequences containing three non-consecutive thymine nucleobases, (e.g., 1.52 and 1.54, respectively, for 5′-AAATTGTGGCCC-3′ and 5′-CCCTTGTGGAAA-3′ oligonucleotide ions). As noted above, intermolecular proton transfers between NH_4^+ and the ssDNA are guided by thermochemical properties (e.g., $\Delta G°_{app}$[acid] including electrostatic effects). Thus, they are also oriented by the proximity of other positive and negative charged sites, which will locally influence the activation energy required for a potential intermolecular proton exchange. For 12-mer ssDNA sequences containing consecutive thymine nucleobases (i.e., 5′-GGGCCACAATTT-3′ and 5′-TTTCCACAAGGG-3′), when one of the phosphate groups directly linked to a thymidine unit (most acidic site of the DNA sequence) already holds a negative charge, the energy required to stabilize another negative charge on an adjacent phosphate group directly linked to a second thymidine unit is raised, and this neighboring anion formation is thereby disfavored. Therefore, despite the relatively high acidity of phospho-thymidine units, the close proximity of several will disfavor the consecutive departures of NH_4^+ cations for a 12-mer and, instead, will achieve a balance wherein the departure of neutral NH_3 molecules becomes more competitive, consistent with previously postulated ESI mechanisms describing desorption/ionization of ssDNA into the gas phase [43].

The above 12-mer example shows that local electrostatic effects can exert influence on the dominant orientation given by gas-phase acidity considerations on the supercharging phenomenon. The situation becomes even more complicated when considering the supercharging of 6-mers where the largest difference in the enhanced charging ($CEC_{1\%}$ values) occurs for 5′-TTATTT-3′ (dispersed thymine nucleobases,

Table 2. Average Charge State (z_{avg}), Highest Observed Charge States (z_{high}) Obtained Without or with Introduction of 1 % of m-NBA in Various ssDNA Solutions; Calculated Charge Enhancement Coefficient ($CEC_{1\%}$), Defined as z_{avg} in the Presence of 1 % of m-NBA Minus z_{avg} in Absence of m-NBA. Relative Standard Deviations (RSD) were Calculated from 10 Different Measurements

	0 % m-NBA			1 % m-NBA			$CEC_{1\%}$	RSD
	z_{avg}	RSD	z_{high}	z_{avg}	RSD	z_{high}		
6-mer								
5′-TTTTTT-3′	2.00	± 0.1 %	2	3.17	± 1.5 %	5	1.17	± 4.5 %
5′-TTATTT-3′	2.00	± 0.1 %	2	3.17	± 0.3 %	5	1.18	± 1.0 %
5′-TTCTTT-3′	2.00	± 0.1 %	2	3.19	± 0.3 %	5	1.19	± 0.9 %
5′-GTTTTT-3′	2.00	± 0.1 %	2	3.36	± 0.2 %	5	1.36	± 0.7 %
5′-GGGTTT-3′	2.04	± 0.1 %	3	3.27	± 0.2 %	5	1.23	± 0.5 %
12-mer								
5′-AAAAACCAAAAA-3′	2.88	± 0.1 %	4	4.22	± 0.2 %	7	1.34	± 0.7 %
5′-GGAA**TT**AACCAA-3′	3.04	± 0.1 %	4	4.52	± 0.1 %	8	1.49	± 0.5 %
5′-CCAA**TT**AAGGAA-3′	3.05	± 0.1 %	4	4.49	± 0.4 %	8	1.43	± 1.9 %
5′-GGGCCACAA**TTT**-3′	3.17	± 0.1 %	4	4.56	± 0.3 %	7	1.38	± 1.2 %
5′-**TTT**CCACAAGGG-3′	3.16	± 0.1 %	4	4.56	± 0.2 %	7	1.41	± 1.0 %
5′-AAA**TT**G**T**GGCCC-3′	3.09	± 0.2 %	4	4.62	± 0.2 %	8	1.52	± 1.0 %
5′-CCC**TT**G**T**GGAAA-3′	3.23	± 0.1 %	4	4.76	± 0.2 %	8	1.54	± 1.2 %
5′-**TT**GG**TT**AA**TT**CC-3′	3.12	± 0.1 %	4	4.71	± 0.3 %	8	1.59	± 1.4 %
5′-GG**TT**AA**TT**CC**TT**-3′	3.13	± 0.1 %	4	4.73	± 0.2 %	8	1.60	± 0.9 %

lowest $CEC_{1\%}$) and 5′-GTTTTT-3′ (dense thymine nucleobases, highest $CEC_{1\%}$) even though each has an identical number of thymines. Thus, in the case of these T-rich 6-mer ssDNA, a high "density" of thymine actually leads to a higher $CEC_{1\%}$. The electrostatic effect that seems to come to the forefront in this case is that preferential protonation of the guanine nucleobase (highest GB) occurring in the aggregate apparently facilitates negative charge formation at the nearest phosphate group. During further desolvation, this proton can be lost as solvent molecules depart, thus leaving only negative charges on the ssDNA that now is a highly charged anion. The above 6-mer containing the adenine nucleobase (lower GB) apparently cannot exhibit the same level of electrostatic influence. Thus, this example shows that the deleterious effect of adjacent deprotonable sites can be overcome by other electrostatic effects that promote deprotonation.

The same rationale can explain why 5′-GTTTTT-3′ has a higher $CEC_{1\%}$ value (1.36) than 5′-TTTTTT-3′ (1.22) even though the former has one fewer thymine nucleobase. Compared with these two, 5′-TTCTTT-3′ ($CEC_{1\%}$ = 1.19) and TTATTT ($CEC_{1\%}$ = 1.16) exhibit slightly lower $CEC_{1\%}$ values, which is in agreement with our proposed model, but only 5′-GGGTTT-3′ (with the T-poorest sequence) gives a $CEC_{1\%}$ = 1.23 that appears to be unusually high, again pointing toward a special role that guanine appears to play in the supercharging process.

Conclusion

m-NBA reagent was already known for favoring protonation of proteic biomolecules in positive ESI mode but it was shown here to promote deprotonation of various ssDNA sequences in negative mode during the ESI desolvation process. Using oligonucleotides as tools to scrutinize the underlying aspects of ESI fundamentals (e.g., transfer and desolvation of ions into the gas phase), m-NBA-induced charge enhancement of oligonucleotide ions in negative ESI mode is thus established. A model emphasizing the role of apparent gas-phase acidity has been proposed to rationalize the phenomenon of supercharging. Particular features examined are (1) the number of thymines, (2) the dispersion of thymines, and (3) the presence of protonable nucleobases (especially guanine). Each of these three components can apparently exert variable electrostatic effects on the overall tendency for charged site formation. The ability to produce more highly charged precursor oligonucleotide ions (induced by the presence of m-NBA) could provide a means to obtain more extensive ion fragmentations in tandem mass spectrometry experiments. This would thereby improve the relevance of fitness values obtained in automated tandem mass spectral sequencing of small oligonucleotides using, for example, the COMPAS, or other similar algorithms [65, 66]. Although no real consensus has yet emerged concerning the mechanism of supercharging in ESI, the current contribution is proposed as an additional brick in constructing a foundation to explain the mechanism of supercharging for both ESI ion modes.

Acknowledgments

Financial support from SANOFI, CEA, the CNRS and the University Pierre and Marie Curie are gratefully acknowledged. The platform SM^3P is also acknowledged.

References

1. Fenn, J.B., Mann, M., Meng, C.K., Wong, S.F., Whitehouse, C.M.: Electrospray ionization for mass spectrometry of large biomolecules. Science **246**(4926), 64–71 (1989)
2. Li, Y., Cole, R.B.: Electrospray and MALDI mass spectrometry, 2nd ed. In: Cole, R.B., (Ed.) Charge State Distributions in Electrospray and MALDI, pp. 491–534. John Wiley and Sons, Inc., Hoboken, New Jersey (2010)
3. Chowdhury, S.K., Katta, V., Chait, B.T.: Probing conformational changes in proteins by mass spectrometry. J. Am. Chem. Soc. **112**, 9012–9013 (1990)
4. Wang, G., Cole, R.B.: Disparity between solution-phase equilibria and charge state distributions in positive-ion electrospray mass spectrometry. Org. Mass Spectrom. **29**, 419–427 (1994)
5. Le Blanc, J.C.Y., Wang, J., Guevremont, R., Siu, K.: Electrospray mass spectra of protein cations formed in basic solutions. Org. Mass Spectrom. **29**, 587–593 (1994)
6. Felitsyn, N., Peschke, M., Kebarle, P.: Origin and number of charges observed on multiply-protonated native proteins produced by ESI. Int. J. Mass Spectrom. **219**, 39–62 (2002)
7. McLuckey, S.A., Van Berkel, G.J., Glish, G.L.: Reactions of dimethylamine with multiply charged ions of cytochrome *c*. J. Am. Chem. Soc. **112**, 5668–5670 (1990)
8. McLuckey, S.A., Glish, G.L., Van Berkel, G.J.: Charge determination of product ions formed from collision-induced dissociation of multiply protonated molecules via ion/molecule reactions. Anal. Chem. **63**, 1971–1978 (1991)
9. Takayama, M., Fukai, T., Nomura, T.: Effect of a new matrix system for low-polar organic compounds in fast atom bombardment mass spectrometry. Shisuryo Bunseki **36**(4), 169–173 (1988)
10. Siuzdak, G., Wendeborn, S.V., Nicolaou, K.C.: Cationization of organometallic carbonyl compounds by fast ion bombardment. Int. J. Mass Spectrom. Ion Processes **112**(1), 79–91 (1992)
11. Reynolds, J.D., Cook, K.D., Burn, J.L.E., Woods, C.: *m*-Nitrobenzyl alcohol electrochemistry in fast atom bombardment mass spectrometry. J. Am. Soc. Mass Spectrom **3**, 113–121 (1992)
12. Ahn, Y.M., Lee, W.-W., Jung, J.H., Lee, S.-G., Hong, J.: Structural determination of glucosylceramides isolated from marine sponge by fast atom bombardment collision-induced dissociation linked scan at constant B/E. J. Mass. Spectrom. **44**, 1698–1708 (2009)
13. Iavarone, A.T., Jurchen, J.C., Williams, E.R.: Supercharged protein and peptide ions formed by electrospray ionization. Anal. Chem. **73**, 1455–1460 (2001)
14. Iavarone, A.T., Williams, E.R.: Supercharging in electrospray ionization: effects on signal and charge. Int. J. Mass Spectrom. **219**, 63–72 (2002)
15. Iavarone, A.T., Williams, E.R.: Mechanism of charging and supercharging molecules in electrospray ionization. J. Am. Chem. Soc. **125**, 2319–2327 (2003)
16. Iavarone, A.T., Williams, E.R.: Collisionally activated dissociation of supercharged proteins formed by electrospray ionization. Anal. Chem. **75**, 4525–4533 (2003)
17. Gorshkov, M.V., Masselon, C.D., Nikolaev, E.N., Udseth, H.R., Pasa-Tolic, L., Smith, R.D.: Considerations for electron capture dissociation efficiency in FTICR mass spectrometry. Int. J. Mass Spectrom. **234**, 131–136 (2004)
18. Zubarev, R.A., Witt, M., Baykut, G.: Two-fold efficiency increase by selective excitation of ions for consecutive activation by ion-electron reactions and vibrational excitation in tandem Fourier transform ion cyclotron resonance mass spectrometry. Anal. Chem. **77**, 2992–2996 (2005)
19. McFarland, M.A., Chalmers, M.J., Quinn, J.P., Hendrickson, C.L., Marshall, A.J.: Evaluation and optimization of electron capture dissociation efficiency in fourier transform ion cyclotron resonance mass spectrometry. J. Am. Soc. Mass Spectrom. **16**, 1060–1066 (2005)
20. Kjeldsen, F., Giessing, A.M.B., Ingrell, C.R., Jensen, O.N.: Peptide sequencing and characterization of post-translational modifications by enhanced

ion-charging and liquid chromatography electron-transfer dissociation tandem mass spectrometry. Anal. Chem. **79**, 9243–9252 (2007)
21. Lomeli, S.H., Yin, S., Loo, R.R., Loo, J.A.: Increasing charge while preserving noncovalent protein complexes for ESI-MS. J. Am. Soc. Mass Spectrom. **20**, 593–596 (2009)
22. Sterling, H.J., Williams, E.R.: Origin of supercharging in electrospray ionization of noncovalent complexes from aqueous solution. J. Am. Soc. Mass Spectrom. **20**, 1933–1943 (2009)
23. Lomeli, S.H., Peng, I.X., Yin, S., Loo, R.R., Loo, J.A.: New reagents for increasing ESI multiple charging of proteins and protein complexes. J. Am. Soc. Mass Spectrom. **21**, 127–131 (2010)
24. Sterling, H.J., Daly, M.P., Feld, G.K., Thoren, K.L., Kintzer, A.F., Krantz, B.A., Williams, E.R.: Effects of supercharging reagents on noncovalent complex structure in electrospray ionization from aqueous solutions. J. Am. Soc. Mass Spectrom. **21**, 1762–1774 (2010)
25. Valeja, S.G., Tipton, J.D., Emmett, M.R., Marshall, A.G.: New reagents for enhanced liquid chromatographic separation and charging of intact protein ions for electrospray ionization mass spectrometry. Anal. Chem. **82**, 7515–7519 (2010)
26. Sterling, H.J., Williams, E.R.: Real-time hydrogen/deuterium exchange kinetics via supercharged electrospray ionization tandem mass spectrometry. Anal. Chem. **82**, 9050–9057 (2010)
27. Hogan Jr., C.J., Loo, R.R., Loo, J.A., de la Mora, J.F.: Ion mobility-mass spectrometry of phosphorylase B ions generated with supercharging reagents but in charge-reducing buffer. Phys. Chem. Chem. Phys. **12**, 13476–13483 (2010)
28. Sterling, H.J., Cassou, C.A., Trnka, M.J., Burlingame, A.L., Krantz, B.A., Williams, E.R.: The role of conformational flexibility on protein supercharging in native electrospray ionization. Phys. Chem. Chem. Phys. **13**, 18288–18296 (2011)
29. Douglass, K.A., Venter, A.R.: Investigating the role of adducts in protein supercharging with sulfolane. J. Am. Soc. Mass Spectrom. **23**, 489–497 (2012)
30. Kebarle, P., Peschke, M.: On the mechanisms by which the charged droplets produced by electrospray lead to gas phase ions. Anal. Chim. Acta **406**, 11–35 (2000)
31. Kebarle, P.: A brief overview of the present status of the mechanisms involved in electrospray mass spectrometry. J. Mass Spectrom. **35**, 804–817 (2000)
32. CRC Handbook of Chemistry and Physics. In [Online] 89th ed., Lide, D.R. (Ed.) (2008–2009)
33. Yin, S., Loo, J.A.: Top-down mass spectrometry of supercharged native protein–ligand complexes. Int. J. Mass Spectrom. **300**, 118–122 (2011)
34. Miladinovic, S.M., Fornelli, L., Lu, Y., Piech, K.M., Girault, H.H., Tsybin, Y.O.: In-spray supercharging of peptides and proteins in electrospray ionization mass spectrometry. Anal. Chem. **84**, 4647–4651 (2012)
35. Kharlamova, A., Prentice, B.M., Huang, T.-Y., McLuckey, S.A.: Electrospray droplet exposure to gaseous acids for the manipulation of protein charge state distributions. Anal. Chem. **82**, 7422–7429 (2010)
36. Brahim, B., Alves, S., Cole R.B., Tabet J.-C.: Signal and charge enhancement of DNA single strands in negative electrospray ionization using the supercharging reagent meta-nitrobenzylalcohol. Proceedings of the ASMS 60th Conference on Mass Spectrometry and Allied Topics, Thursday Poster 201. Vancouver, 20–24 May (2012)
37. Limbach, P.A., Crain, P.F., McCloskey, J.A.: Characterization of oligonucleotides and nucleic acids by mass spectrometry. Curr. Opin. Biotechnol. **6**, 96–102 (1995)
38. Crain, P.F., McCloskey, J.A.: Applications of mass spectrometry to the characterization of oligonucleotides and nucleic acids. Curr. Opin. Biotechnol. **9**, 25–34 (1998)
39. Esmans, E.L., Broes, D., Hoes, I., Lemiere, F., Vanhoutte, K.: Liquid chromatography-mass spectrometry in nucleoside, nucleotide, and modified nucleotide characterization. J. Chromatogr. A **794**, 109–127 (1998)
40. Wu, J., McLuckey, S.A.: Gas-phase fragmentation of oligonucleotide ions. Int. J. Mass Spectrom. **237**, 197–241 (2004)
41. Alves, S., Woods, A., Tabet, J.-C.: Charge state effect on the zwitterion influence on stability of non-covalent interaction of single-stranded DNA with peptides. J. Mass Spectrom. **42**, 1613–1622 (2007)
42. Banoub, J.H., Newton, R.P., Esmans, E., Ewing, D.F., Mackenzie, G.: Recent developments in mass spectrometry for the characterization of nucleosides, nucleotides, oligonucleotides, and nucleic acids. Chem. Rev. **105**, 1869–1915 (2005)
43. Rosu, F., Pirotte, S., De Pauw, E., Gabelica, V.: Positive and negative ion mode ESI-MS and MS/MS for studying drug-DNA complexes. Int. J. Mass Spectrom. **253**, 156–171 (2006)
44. Sannes-Lowery, K.A., Mack, D.P., Hu, P.F., Mei, H.Y., Loo, J.A.: Positive ion electrospray ionization mass spectrometry of oligonucleotides. J. Am. Soc. Mass Spectrom. **8**, 90–95 (1997)
45. Boschenok, J., Sheil, M.M.: Electrospray tandem mass spectrometry of nucleotides. Rapid Commun. Mass Spectrom. **10**, 144–149 (1996)
46. Vrkic, A.K., O'Hair, R.A.J., Foote, S., Reid, G.E.: Fragmentation reactions of all 64 protonated trimer oligodeoxynucleotides and 16 mixed base tetramer oligodeoxynucleotides via tandem mass spectrometry in an ion trap. Int. J. Mass Spectrom. **194**, 145–164 (2000)
47. Wang, P.P., Bartlett, M.G., Martin, L.B.: Electrospray collision-induced dissociation mass spectra of positively charged oligonucleotides. Rapid Commun. Mass Spectrom. **11**, 846–856 (1997)
48. Weimann, A., Iannitti-Tito, P., Sheil, M.M.: Characterization of product ions in high-energy tandem mass spectra of protonated oligonucleotides formed by electrospray ionisation. Int. J. Mass Spectrom. **194**, 269–288 (2000)
49. Hakansson, K., Hudgins, R.R., Marshall, A.G., O'Hair, R.A.J.: Electron capture dissociation and infrared multiphoton dissociation of oligodeoxynucleotide dications. J. Am. Soc. Mass Spectrom. **14**, 23–41 (2003)
50. Alves, S., Woods, A., Delvolve, A., Tabet, J.-C.: Influence of salt bridge interactions on the gas-phase stability of DNA/peptide complexes. Int. J. Mass Spectrom. **278**, 122–128 (2008)
51. Hunter, E.P., Lias, S.G.: Evaluated gas phase basicities and proton affinities of molecules: an update. J. Phys. Chem. Ref. Data **27**(3), 413–656 (1998)
52. Griffey, R.H., Sasmor, H., Greig, M.J.: Oligonucleotide charge states in negative ionization electrospray-mass spectrometry are a function of solution ammonium ion concentration. J. Am. Soc. Mass Spectrom. **8**, 155–160 (1997)
53. Favre, A., Gonnet, F., Tabet, J.-C.: Location of negative charges of single-stranded DNA in the gas phase. Eur. J. Mass Spectrom. **6**, 389–396 (2000)
54. Greco, F., Liguori, A., Sindona, G., Uccella, N.: Gas-phase proton affinity of deoxyribonucleosides and related nucleobases by fast atom bombardment tandem mass spectrometry. J. Am. Chem. Soc. **11**, 9092–9096 (1990)
55. Strittmatter, E.F., Schnier, P.D., Klassen, J.S., Williams, E.R.: Dissociation energies of deoxyribose nucleotide dimer anions measured using blackbody infrared radiative dissociation. J. Am. Soc. Mass Spectrom. **10**, 1095–1104 (1999)
56. Xu, Y., Afonso, C., Gimbert, Y., Fournier, F., Dong, X., Wen, R., Tabet, J.-C.: Gas phase self-association of Eudistomin U controlled by gas phase acidity and origin of its interaction with nucleobases. Int. J. Mass Spectrom. **286**, 43–52 (2009)
57. Madsen, J.A., Brodbelt, J.S.: Asymmetric charge partitioning upon dissociation of DNA duplexes. J. Am. Soc. Mass Spectrom. **21**, 1144–1150 (2010)
58. Gidden, J., Bowers, M.T.: Gas-phase conformations of deprotonated trinucleotides (dGTT$^-$, dTGT$^-$, and dTTG$^-$): the question of Zwitterion formation. J. Am. Soc. Mass Spectrom. **14**, 161–170 (2003)
59. Robertazzi, A., Platts, J.A.: Gas-phase DNA oligonucleotide structures, a QM/MM and atoms in molecules study. J. Phys. Chem. A **110**, 3992–4000 (2006)
60. Balbeur, D., Widart, J., Leyh, B., Cravello, L., De Pauw, E.: Detection of oligonucleotide gas-phase conformers: H/D exchange and ion mobility as complementary techniques. J. Am. Soc. Mass Spectrom. **19**, 938–946 (2008)
61. Hardman, M., Makarov, A.A.: Interfacing the Orbitrap mass analyzer to an electrospray ion source. Anal. Chem. **75**, 1699–1705 (2003)
62. Olsen, J.V., de Godoy, L.M.F., Li, G., Macek, B., Mortensen, P., Peach, R., Makarov, A., Lange, O., Horning, S., Mann, M.: Parts per million mass accuracy on an Orbitrap mass spectrometer via lock mass injection into a C-trap. Mol. Cell. Proteom. **4**(12), 2010–2021 (2005)
63. Hu, Q., Noll, R.J., Li, H., Makarov, A., Hardman, M., Cooks, R.G.: The Orbitrap: a new mass spectrometer. J. Mass Spectrom. **40**, 430–443 (2005)
64. Wang, G., Cole, R.B.: Effect of solution ionic strength on analyte charge state distributions in positive and negative ion electrospray mass spectrometry. Anal. Chem. **66**, 3702–3708 (1994)
65. Oberacher, H., Oefner, P.J., Mayr, B.M., Huber, C.G., Parson, W.: Applicability of tandem mass spectrometry to the automated comparative sequencing of long-chain oligonucleotides. J. Am. Soc. Mass Spectrom. **15**, 510–522 (2004)
66. Oberacher, H., Pitterl, F.: On the use of ESI-QqTOF-MS/MS for the comparative sequencing of nucleic acids. Biopolymers **91**, 401–409 (2009)